Ind. J. Pharm. Edu. Res., 2026; 60(2s):s443-s461.
https://www.ijper.org

Original Article

Design and Development of Chitosan-Based Posaconazole Loaded Dry Powder by Using BBD

Sushil Kumar Singh[1], Shyam Sunder Pancholi[2,*]

[1]Department of Pharmaceutical Technology, Ganpat University, Kherva, Mehsana, Gujarat, INDIA.
[2]Department of Pharmaceutics, School of Pharmacy and Technology Management (SPTM) SVKM's NMIMS (Deemed to be University) Mukesh Patel Technology Park, Babulde, Shirpur, Dhule, Maharashtra, INDIA.

ABSTRACT

Aim: Quality by Design (QbD)-Optimized Spray-Dried Microparticles (prepared by using spray drying process) of Posaconazole-Loaded Chitosan Nanoparticles (POS-CSNPs) for enhanced antifungal efficacy. **Materials and Methods:** Box-Behnken Design (BBD) a systematic design of experiments was implemented, to screen and optimize the formulation variables for the intended qualities. **Results:** Outcomes showed that POS-CSNPs have particle size (259.33±6.82 nm), Poly dispersity Index (0.192±0.010), zeta potential (-31.23±0.84 mV) and %Entrapment Efficiency (65.17±1.71). *In vitro* fungal study result showed the enhanced antifungal and higher fungicidal effect on *Rhizopus oryzae* strains. **Conclusion:** From the result it is concluded that the preparation of POS-CSNPs have higher anti-fungal effect on fungus strain.

Keywords: Box-Behnken design, Dry powder Inhaler, *In vitro* Fungal study, Nanoparticles, Posaconazole.

Correspondence:
Dr. Shyam Sunder Pancholi
Professor and Associate Dean, Department of Pharmaceutics, School of Pharmacy and Technology Management (SPTM), SVKM's NMIMS (Deemed to be University), Mukesh Patel Technology Park, Babulde, Shirpur-425405, Dhule, Maharashtra, INDIA.
Email: sspancholi@gmail.com

Received: 04-08-2025;
Revised: 29-09-2025;
Accepted: 03-11-2025.

INTRODUCTION

The main ailment of pulmonary mucormycosis is a serious fungal infection that can be fatal. The majority of cases are caused by Mucor, Rhizopus, and Lichtheimia, which are the most common Mucorales species.[1] It is classed as an opportunistic angio-invasive fungal infection. This infection is more common in those who are immunocompromised, such as those receiving immunosuppressive medication, have uncontrolled diabetes, or have hematological malignancies. But immunocompetent persons have also been documented to have pulmonary mucormycosis, demonstrating the wide range of people who might be affected.[2,3]

Because of its unspecific clinical presentation and the difficulties in getting reliable test data, pulmonary mucormycosis can be difficult to diagnose, particularly in immunocompromised individuals. The diagnosis of this illness might be complicated by the fact that it can present with symptoms that are similar to other lung fungal diseases, such as Aspergillosis. Due to the high death rates associated with pulmonary mucormycosis, particularly in certain groups such as patients of kidney transplants, early identification is essential. A multidisciplinary strategy is frequently used to treat pulmonary mucormycosis, and it may require antifungal medication as well as occasionally surgical intervention.[4,5]

In the United States and the United Kingdom, aspergillosis, candidiasis, and other invasive fungal infections in people over the age of 13 can be treated with posaconazole, a structural counterpart of itraconazole, which was authorized in 2005 and 2006. The oral solution, intravenous injections, and delayed-release tablets are the three posaconazole formulations that are currently officially approved.[6,7]

The second-generation triazole antifungal drug posaconazole has become well-known for its strong and widespread antifungal action. Treatment for Rhizopus species-caused pulmonary mucormycosis with posaconazole has been shown effective. Furthermore, improvements in fungus clearance in experimental models of pulmonary mucormycosis have been achieved with the application of IFN-γ mediated signaling. It works by blocking lanosterol 14α-demethylase (CYP51), which prevents ergosterol from being synthesized, which is an essential part of the fungal cell membrane. This, in turn, prevents fungal cell growth (disturbance results in impaired membrane stability) and precursor accumulation, which has fungistatic or fungicidal effects.[8-10]

The drug posaconazole comes in a variety of commercially accessible forms, such as oral solution and delayed-release pills. Its low solubility and limited bioavailability provide a number of issues and obstacles, and its adverse effects might include

DOI: 10.5530/ijper.20261364

headaches, nausea, vomiting, diarrhea, stomach discomfort, and rash. Atypical cardiac rhythms, allergic responses, and liver issues are examples of uncommon but potentially serious adverse effects.[11,12]

A viable approach to preventing pulmonary fungal infections is the use of Dry Powder Inhalers (DPIs), which possess the capacity to lessen systemic adverse consequences, increase patient compliance, and deliver targeted drug delivery to the respiratory system (aerodynamic spaces). One advantage of using aerosolized antifungal medications is that they can more quickly reach the infection site, improving the efficacy of treatment. Because this approach doesn't require needles or intrusive procedures, it is convenient for patients. It's also less likely to cause adverse effects in other bodily areas, which makes it a safer choice. Additional study information would be required to discuss certain conclusions and their ramifications. Making Posaconazole into lipid-based nanocarriers like liposomes or nano-emulsions is one noteworthy method. They have addressed issues related to the drug's low water solubility and increased its therapeutic effectiveness by demonstrating better bioavailability and sustained release. Nanoparticles have a high degree of adaptability in pharmaceutical applications by having the ability to increase medication penetration and the antimicrobial activity of pharmaceuticals.[13-16]

It fully understands how procedure parameters relate to one another in order to achieve the required ideal overall product quality characteristics. BBD is used for the synthesis and refining the CS nanoparticle loaded with POS. As a result, a better POS-loaded CS nanoparticle are produced. In order to guarantee optimization, the QBD approach was employed during the development phase. A workable technique for producing polymeric nanoparticulate systems is ionotropic gelation. This method has been reported in several investigations, where different medications are encapsulated within the polymeric nanoparticles utilizing Tripolyphosphate (TPP), the countercharged component, and chitosan, a naturally cationic polymer.[17-19]

Furthermore, chitosan's mucoadhesive qualities help to extend the duration of drug residence and regulate drug release in the lungs, which increases its applicability for pulmonary drug delivery applications. Investigating other tactics has become necessary in order to overcome issues such excessive aggregation and early exhalation that arise from using nanoparticles for inhalation on their own. A possible approach is to use particle engineering methods such as spray drying to generate nanoparticle-containing dry powders at the micron scale.[20,21]

This methodology tackles the problem of nanoparticle aggregation and advances the development of stable solid-state formulations, so augmenting the prospects for efficient and regulated drug administration in inhalation treatments. When making inhalable dry powder nanoparticles, adding carriers like lactose makes it easier to get the right median aerodynamic diameter for optimal alveolar deposition. It guarantees a more consistent and effective pulmonary medication delivery mechanism by preventing aggregation. This work sought to clarify a method for using the ionic gelation process to create POS-loaded CS-nanoparticles. By adding a Tripolyphosphate (TPP) solution, which has a pH range of 6-9, to an acidic chitosan solution, which has a pH range of 4-6, one may typically create nanoparticles using this approach. This approach is important for attaining desirable drug encapsulation and nanoparticle properties since the well-managed pH conditions are essential to the effective production of nanoparticles.[22-24]

This study focused on the crucial ratio of chitosan to TPP, which is closely related to the pH of the solution. Because Posaconazole (POS) has very little water solubility, a compound of POS-HPβCD was used in all of the tests. In order to preserve the drug's high solubility, this combination was first incorporated into chitosan-TPP nanoparticles. This was made possible by the nanoparticles' larger surface area than that of inhalable microparticles. Notably, the medication had to be dissolved and the POS-HPβCD complex had to form in order to generate chitosan/TPP nanoparticles at a pH as low as 1.2 to 1.4. It was necessary to carefully control the ratio of TPP to chitosan due to the unusual pH range of 1.2-1.4 while making chitosan nanoparticles using the ionic gelation technique.[25]

Factor interactions cannot be ascertained using traditional techniques of testing and optimization since they only take into account one variable at a time. The ICH (Q8) standards have recently proposed Quality by Design (QbD) as a way to improve crucial process parameters in order to achieve the goal quality in the product. The method of Design of Experimentation (DoE) begins with predefined goals and concentrates on improving comprehension of process parameters and product design. Moreover, the link between independent variables (factors) and dependent variables (responses) is correlated using DoE. With fewer tests and the added benefit of allowing for data extrapolation through charting, DoE yields more dependable findings. To determine the response of independent factors for the optimization of pharmaceutical formulations, a response surface technique has been investigated. With a minimal run of tests among several design alternatives, the Box-Benhken design is the most widely used design.[26-28]

Next the research investigated the physical and aerosolization features of the microparticles that were created by spray-drying lactose-laden CS-nanoparticles loaded with Hydroxypropyl-β-Cyclodextrin (HPβCD) and Posaconazole (POS). In order to maximize the benefits of POS-loaded microparticle distribution and the aerosolization characteristics of the microparticles in a synergistic manner, co-spray drying with these excipients has become a viable strategy. Our current study is to clarify the steps involved in creating and constructing Posaconazole (POS)

microparticles using spray drying technology. The CS-NPs with lactose (Microparticles) including POS preparations were examined for several characterisation criteria. Fluorescence microscopy was used for the qualitative localization investigation. Ryazopus oryzae was used as a test subject for fungicidal and targetability assessments. The created formulations were also tested *in vitro* on different fungal species, yielding results for fungus study.

MATERIALS AND METHODS

The drug Posaconazole (POS) purchased from Neuland Laboratories Limited in Hyderabad, India. 90% deacetylated, medium molecular-weight chitosan brought from Sigma Life Science in India. Lactose India Limited, India, generously provided the lactose. HPβCD bought from Sigma in the UK. Inactive ingredients like; Tripolyphosphate Pentasodium salt (TPP), glacial acetic acid, NaOH and all solvents in analytical grades and HPLC grades were brought by Merck Co., Germany. The additional solvents, including methanol, obtained from Thermo Fisher Scientific India Pvt. Ltd., Powai, located in Mumbai, India.

Instrument

Spray Dryer Model SPD-P-111 (Techno search Process and Systems Maharashtra, India); High-Performance Liquid Chromatography (Agilent Technologies, Inc.); Differential Scanning Calorimeter -DSC 6000 (Perkin Elmer, Inc.); ATR-FITR (Thermo Scientific, Inc)., Zetasizer® instrument manufactured by Malvern Instruments.

FT-IR analysis of compatibility research

Pharmacological dosage form formulation involves a vital step that is the investigation of drug excipients compatibility.[29] Investigation on the interactions of drugs with a number of excipients used in the development of formulation were conducted to see, if interactions among the drug and excipients could take place to determine how such interactions may impact the stability and properties of the final formulation. This indicates the likelihood that there won't be situations of a similar kind. A drug's incompatibility along with more than one ingredient may compromise a formulation's stability as well as bioavailability of the active component, hence impacting the formulation's efficacy and safety. Thermo FISHER investigated possible interactions between drugs and the excipient using FTIR (FT-IR8400S) analysis. POS, CS, HPβCD, Lactose, TPP, and their equimolar (1 Mm) physical combination were used to scan the infrared region (4000-500 cm^{-1}).

Posaconazole-HPβCD solution and Chitosan: TPP nanoparticle preparation

Posaconazole solution was made by dissolving 100 mg of POS in 50 ml of HPβCD solution (50 mg/ml) for 3-4 hr using magnetic stirring. The solution's pH was lowered to 1.2 by the addition of concentrated hydrochloric acid and ratio shown in Supplementary Table 1.[30] Chitosan-TPP nanoparticles are formed via an ionotropic gelation technique,[31] whereby chitosan and TPP have been used as proportionally positive and negative charges. The final theoretical ratios of chitosan: TPP, which consisted of 1:0.5, 2:1, and 3:1.5 (w/w), were created by first dissolving chitosan and TPP in 1.2 pH filtered water. In the second step, more chitosan was made at TPP ratios ranging from 1:0.5 to 3:1.5 according on the outcomes of the first stage. The POS-HPβCD solution was combined with the chitosan solution to incorporate POS into the nanoparticles. The mixture was progressively mixed in the TPP solution after 10-20 min stirring time. The formulation was also modified using the Box-Behnken design software.

Box Behnken design optimization of CS-NPs (using Response Surface Methodology)

The Box-Behnken Design (BBD) offers several advantages over a full factorial design when it comes to detecting curvature and modeling quadratic effects in Response Surface Methodology (RSM). One of the key benefits is that BBD is more efficient because it requires fewer experimental runs compared to a full factorial design, especially when dealing with three or more factors. This is particularly important in experiments where resources like time or materials are limited. For capturing curvature, BBD is well-suited because it systematically places experimental points in a spherical or rotatable region, ensuring that all points are at mid-level combinations or at the center of the design space. This enables better detection of quadratic effects without requiring extreme high or low levels of the factors, which can be useful for avoiding impractical or unsafe operating conditions. In contrast, factorial designs, particularly full factorials, are more focused on linear and interaction effects and may require additional center points or more extensive replication to detect curvature effectively. Furthermore, the structure of BBD inherently provides robust information about both main effects and interactions, while also offering sensitivity to quadratic effects, which is ideal for developing second-order polynomial models. Overall, BBD is more economical and less exhaustive while maintaining strong predictive power for response surfaces with curvature.

The whole process was optimized through the use of Box-Behnken design response surface methodology with 17 runs, 3 levels, 3 factors, and 5 centered points. Utilizing the Box-Behnken Design (BBD),[32] Design Expert (licensed Version 13, Stat-Ease Inc., MN) software was used to create the experimental design to study the effects of excipients on changing several physicochemical attributes and the biological response of the nanoparticles. Numerous data points were incorporated in these polynomial models, such as those at the multidimensional cube's midpoint, ends, and repeated center point, to guarantee thorough coverage of the experimental space. Using all independent variables integrated into a well-designed experimental framework, this

approach uses the data collected to produce a set of equations that may theoretically predict the intended results. Furthermore, BBD has the benefit of requiring fewer experimental runs than Central Composite Design (CCD) while preserving a consistent variance throughout the design space. The polynomial quadratic model is developed by using the regression using least squares approach in conjunction with ANOVA to estimate the linear, quadratic, and interaction coefficients.

$$Y=\beta_0+\beta_1A+\beta_2B+\beta_3C+\beta_4AB+\beta_5AC+\beta_6BC+\beta_7A^2+\beta_8B^2+\beta_9C^2$$

Here, Y stands for the measured response variables (like PS, % EE, and PDI) associated with every potential pairing of various factor values. The coefficients of regression, which range from β_0

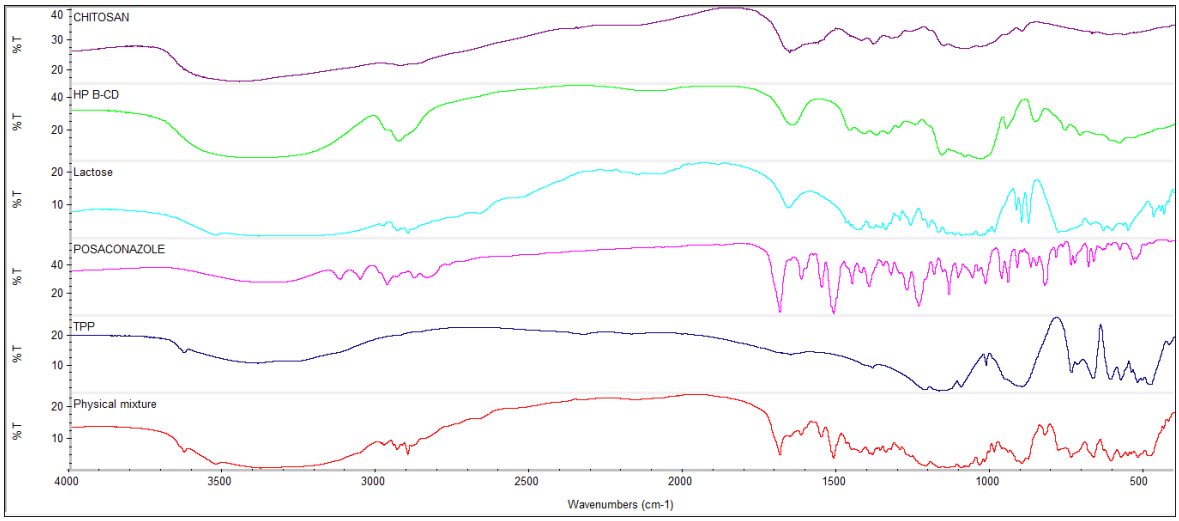

Figure 1: Overlay of Drug-excipients compatibility study by FT-IR spectroscopy.

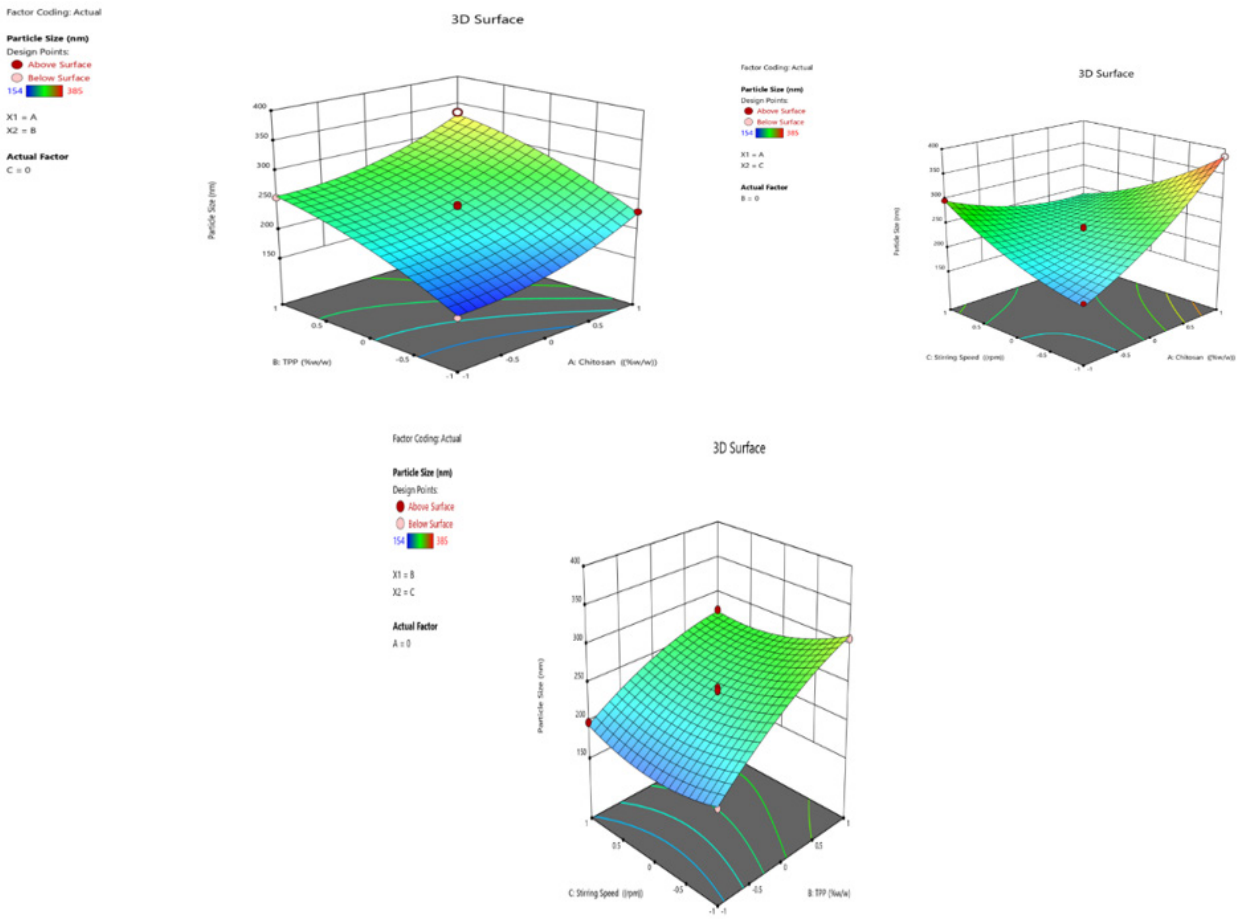

Figure 2 a(i): 3D response surface plot for effect of all independent variables on Chitosan.

to β_9, evaluate the effect of every independent variable (shown as the variables A, B, and C) either by itself or in combination on the model's result.

Three independent factors were chosen: stirring speed, CS: TPP ratio, and Particle Size (PS), Entrapment Effectiveness (EE), and Polydispersity Index (PDI) were assessed as dependent variables (R) (Supplementary Table 2). After 17 experimental runs, the data collected from the desired matrix were carefully analyzed and employed in regression analysis to generate polynomial equations indicating correlations among the components under investigation and the responses.

PDI, Zeta potential, and particle size

The Dynamic Light Scattering (DLS) technique, Analysis was done on the nanoparticles' size. The Polydispersity Index (PDI), zeta potential, and particle size distribution were also measured. Concurrent zeta potential analyses were also carried out using a Beckman Coulter Zetasizer® instruments (Delsa Nano C, USA.[33] Using a 90º detector angle and a helium laser as the light source, scattering was observed during the experiment. The temperature was maintained at 25±0.5ºC. The size of the particles was determined after the nanoparticle solution was diluted 100 times in Phosphate-Buffered Saline (PBS), which has a pH of 7.4. Approximately 3 mL of the sample (diluted) was used for the measurements of Particle Size (PS), Zeta Potential (ZP), and Polydispersity Index (PDI) after it was put into a cuvette. The average of three different data taken for every sample was used to determine the findings.

Determination of Efficiency Entrapment

The drug's entrapment effectiveness for chitosan nanoparticles loaded with it might be indirectly determined by centrifuging the particles in an aqueous solution containing non-encapsulated Posaconazole. This was carried out using an Amicon® ultra centrifugal tube with a molecular weight cut-off of 10 kDa at 6000 rpm for 15 min at 25ºC. The amount of drugs that had been encapsulated was utilizing a UV spectrophotometer (Shimadzu, UV-1900i, Kyoto, Japan) to measure the absorbance at 262 nm. The real quantity of drug encapsulated divided by the total dosage of drugs used to prepare the formulation yielded the encapsulation efficiency percentage or EE%).

Drug entrapment efficiency (%EE)={(Total wt. of drug- wt. of unentrapped drug)/ Total wt. of drug} x 100.

To make sure the results were reliable and consistent; the measurements were done three times.

Study of surface morphology (TEM)

The air-dried sample on the carbon-coated copper grid was then thoroughly and highly resolvedly employing transmission electron microscopy to investigate (EM208S, TEM, Philips CM 10,100 Kv), enabling a closer look at the shape and structure of the nanoparticles. To stain the sample adversely, 1% (w/w) of phosphotungstic acid was then added.[34]

Table 1: Box-Behnken design matrix for the investigation of three experimental elements at coded levels with experimental findings.

Runs	Factor 1 Chitosan %wt/v	Factor 2 TPP %wt/v	Factor 3 Stirring Speed (rpm)	Response 1 Particle Size (nm)	Response 2 EE (%)	Response 3 PDI
1	0	0	0	231	70	0.295
2	-1	0	-1	187	59.4	0.529
3	-1	-1	0	154	39.6	0.177
4	0	0	0	240.9	64.9	0.233
5	0	0	0	239.8	64.9	0.257
6	-1	1	0	255.2	49.5	0.133
7	0	1	-1	308	63.8	0.156
8	-1	0	1	297	55	0.563
9	0	0	0	244.2	66	0.312
10	1	0	1	231	60.5	0.573
11	0	1	1	275	66	0.157
12	0	-1	-1	187	51.7	0.235
13	1	0	-1	385	61.6	0.54
14	1	-1	0	231	44	0.2
15	0	-1	1	198	46.2	0.31
16	0	0	0	236.5	63.8	0.27
17	1	1	0	334.4	57.2	0.199

Analysis of X-ray Diffraction (XRD)

An XRD examination was conducted to check drug loading and ascertain if our formulation of POS-CS microparticles was crystalline or amorphous. The properties of pure POS and spray-dried POS loaded CS nanoparticles with lactose were examined using an Empyrean, Malvern P analytical X-ray diffractometer Samples were placed in the sample stage with an operating voltage of 40 kV and a current of 30 mA and scanned for 2-6 hr.[35]

Table 2:An overview of each of the three responses' ANOVA findings.

Parameters	PS	EE	PDI
p value	<0.0001	<0.0001	<0.0001
F value	171.14	26.30	31.80
Predicted R^2	0.9550	0.8085	0.7691
Adjusted R^2	0.9897	0.9343	0.9454
Adeq Precision	50.7114	15.4630	17.0536
Model	Significant	Significant	Significant
Lack of Fit	Not significant	Not significant	Not significant

DSC thermal analysis

Thermal analysis and melting point determination were performed using an indium-calibrated DSC (PerkinElmer 6000, Massachusetts, USA) to investigate the heat/thermal behavior of the drug (POS), polymer (CS), lactose, TPP, HP-βCD, lactose, and the formulation. 3-5 mg of free drug POS were packed within standard aluminum pans for examination, and spray-dried optimal formulation thermograms were created with a scanning range of 30 to 400°C and 20°C/min as the scanning speed. The phase transition temperature was once used to describe a sample's maximum excess heat capacity.[36]

In vitro drug release

Making use of the dialysis bag method, the *in vitro* POS release profile of the optimized formulations in a substance such as buffer saline (PBS; pH 7.4) was ascertained. Free POS solution and POS-CSNPs suspension were given to every pre-treated dialysis membrane bag (DM MWCO 14 kD; LA-395, Himedia, Mumbai, India) that was handled. The Optimized formulations that contained membranes were immersed in a substance that was kept at 37± 1 ˚C. Every 1, 2, 4, 8, 12, 24, 48, and 60 hr later, samples (1.0 mL) were extracted. and replaced with the similar volume (1.0 mL) of new media. To analyze the POS concentration, the extracted sample portions were subjected to

Table 3: Characterization of the optimized formulations (Mean±SD, i=3).

Formulation	Particle size (nm) (Mean±SD*)	PDI (Mean±SD*)	%EE (Mean±SD*)	ZP (Mean±SD*)
POS-CSNPs	259.33±6.82	0.192±0.010	65.17±1.95	-31.23±0.84

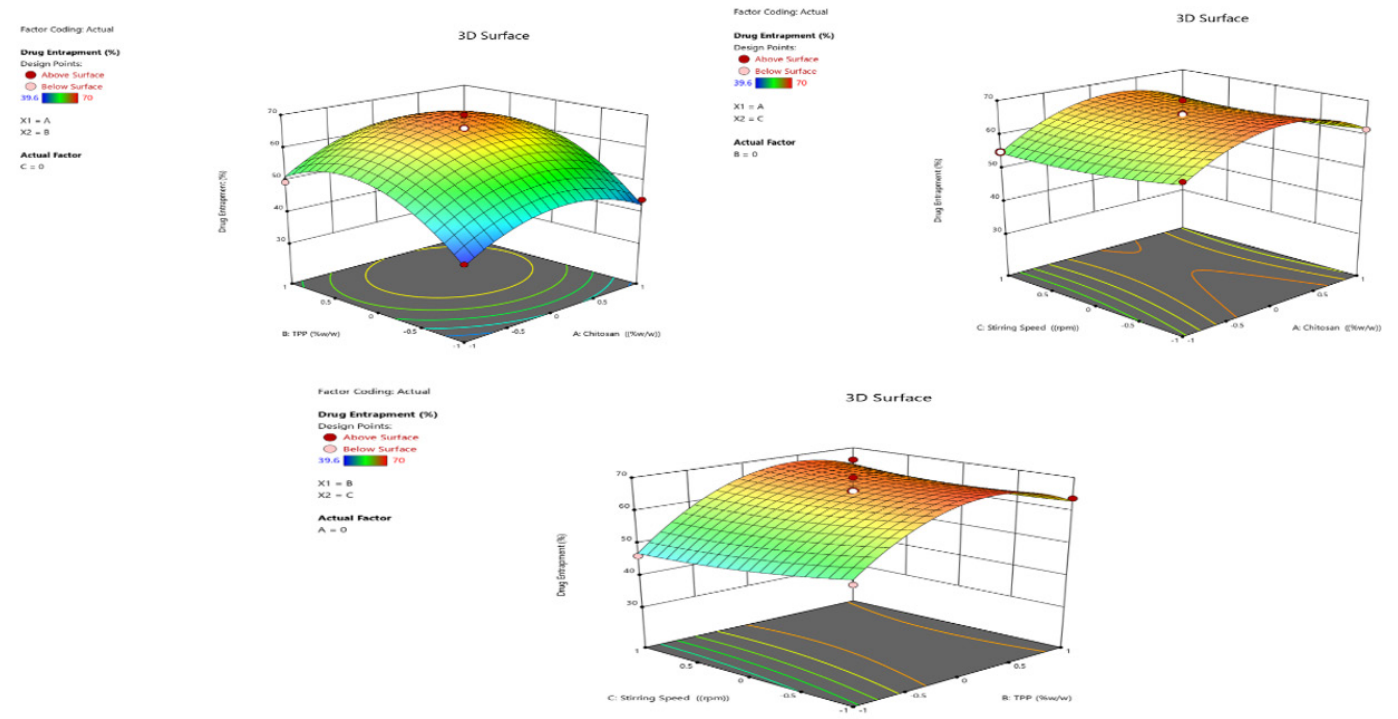

Figure 2 a(ii): 3D response surface plot for effect of all independent variables on Tripolyphosphate (TPP).

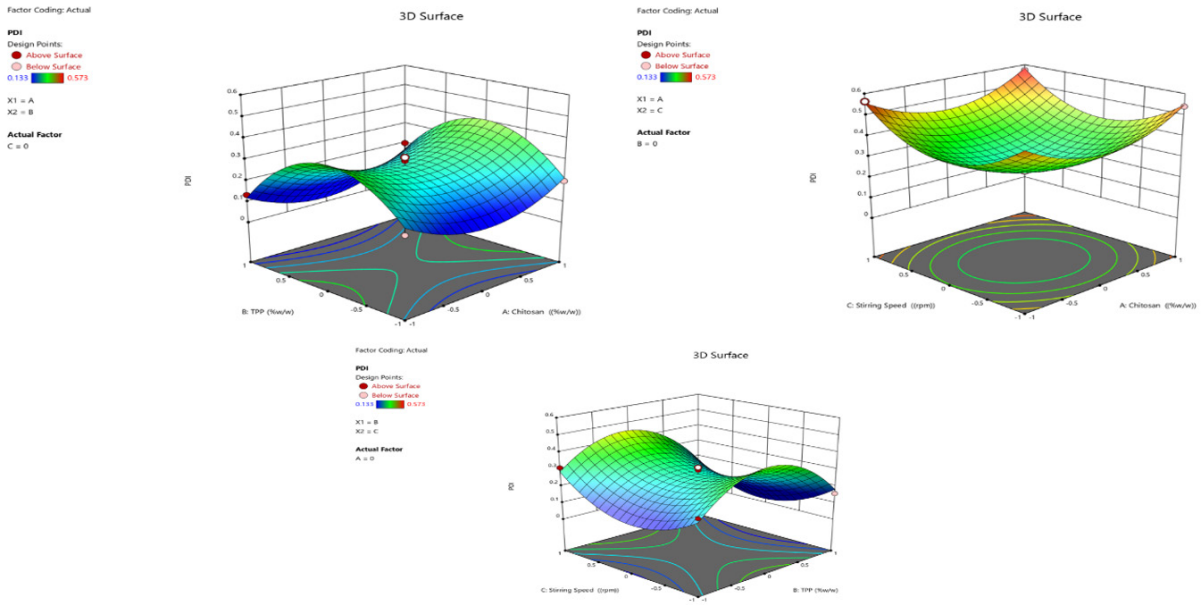

Figure 2 a(iii): 3D response surface plot for effect of all independent variables on Stirring Speed (rpm).

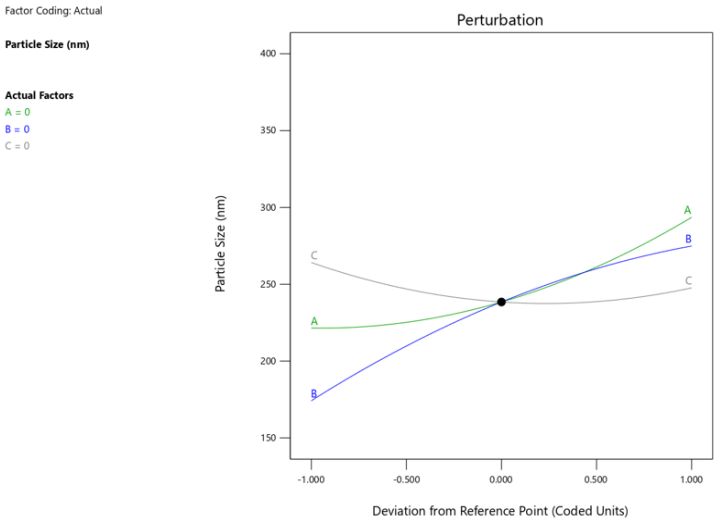

Figure 2 b(i): Perturbation graph for the effect of all independent variables on Particle Size (PS).

UV light at a maximum wavelength of 262 nm using a UV-Vis spectrophotometer (Shimadzu UV-1900i, Kyoto, Japan).[37]

Posaconazole-containing nanoparticles are sprayed dried

The POS-CSNPs sediments were resuspended in lactose-aqueous solutions after centrifugation. The whole weight of the POS-CSNPs was adjusted for 5%, 10%, and 20% lactose (w/w). Spray-drying the excipient and nanoparticle solutions resulted in the formation of dry powders using a small spray-dryer (Techno search procedure and System)[38] and the settings given in Supplementary Table 3. Spraying the suspensions in the same direction using a dual-fluid nozzle that has a 0.7 mm diameter to generate a co-current hot air flow. In order to compare the various formulations, spray-dried POS-CSNPs in an aqueous solution were also employed as a control. Powders were gathered and kept at room temperature in a firmly covered container after spray drying. The weight of powder collected from the spray dryer collection vessel divided by the total solid weight initially used to manufacture each formulation was used to calculate the spray drying process yield for each formulation. To represent this amount, a percentage is utilized.

Size distribution of microparticles that were spray-dried

The Zetasizer® device, made by Malvern Instruments, was used to determine the microparticle size of spray-dried materials using a laser light diffraction technique. In conclusion A same quantity of every sample was distributed uniformly using 5 mL of a suitable dispersion medium (the drug, all excipients,

and absolute ethanol saturated), and it was then sonicated (Starsonic60, Liarre, Italy). Drop by drop, the generated samples were introduced to the instrument cell. The results were expressed using the volume diameter's mode and median. The definition of the span is [D(v,90)-D(v,10)]/D(v,50), where the diameters at 90%, 10%, and 50% cumulative volume are, respectively, represented by D(v,90), D(v,10), and D(v,50). The particle size distribution's spread is measured through its span. The gold-palladium approach was employed in a double-sided tape sputter coating (JEOL equipment) to affix the microparticles to the stubs. Following that, images were taken using the electron microscope JEOL JSM-840 (JEOL USA, Inc.). At a distance of 10 mm, an accelerating voltage of 15 kV was applied.[39]

Content uniformity of the spray-dried microparticles

With some modifications, an acid hydrolysis chitosan approach was applied to evaluate the homogeneity of POS content in the resultant microparticles. In summary, an acidic medium with a pH of 0.6 was used to dissolve 10-m samples of each formulation. The mixture was then heated to 72°C for 30 min while being agitated. To halt the process, submersion in an ice bath was employed. Each sample's POS content was ascertained using the HPLC method. Three measurements were made of each sample.[40]

Study of *in vitro* pulmonary deposition

A twin-stage impinger apparatus (TSI; Copley, UK) was used to study pulmonary drug deposition, and Rotahaler was used as a dry powder inhalation tool.[41] In steps 1 and 2, concentrated HCl solutions with a pH of 0.6 were added. For four seconds, every capsule (size 3) 60 liters per minute of aerosolization. The aerosolization variables are measures as follows: when five capsules containing 45 mg of microparticles are aerosolized, the POS amounts at each TSI and device stage are determined. The FPF (fine particle fraction) was defined as the quantity of medicine deposited in stage 2 of TSI as a percentage of the total amount of medication placed in the capsule. The "Emitted Dose percentage" (ED%) is the amount of drug expelled from the inhaler stated as a percentage of the total dosage of drug contained in the capsule.

In vitro Fungal study

The effectiveness of the optimized formulation against Rhyzopus oryzae fungus strains was investigated using an antifungal investigation. In this investigation, conventional paper discs, sanitized Petri plates, and Sabouraud Dextrose Agar (SDA) medium were utilized. In the sterile Petri plate, SDA (20 mL) given the test organism treatment (0.5 mL) was allowed to harden. Pretreated paper discs (Wattman filter No. 42, 4 mm in diameter) were carefully put on the surface of Sabouraud dextrose agar medium in a sterile manner after being soaked in test solutions (POS, Optimized Formulations). According to Moglad *et al.* (2020), Petri plates were then incubated for 48 hr at 27°C. Using a ruler, Measurements and observations were made of the Zones of Inhibition (ZI) sizes.[42]

Stability analyses

To examine the stability during storage as per ICH guidelines,[43] SD powder of optimized formulations was exposed to accelerated stability conditions (40°C/75%). The SD formulation was placed into gelatin capsules and sealed in HDPE bottles. It was then charged on stability for three months 40°C/75%). The powder's physical properties, the drug content, the particle size, and Poly dispersity Index were the stability conditions and Comparison of Particle size and PDI of freshly prepared POS-CSNPs and redispersed POS-CSNPs.

% Drug content=(Amount of drug present/Total weight of the formulation)x100.[44]

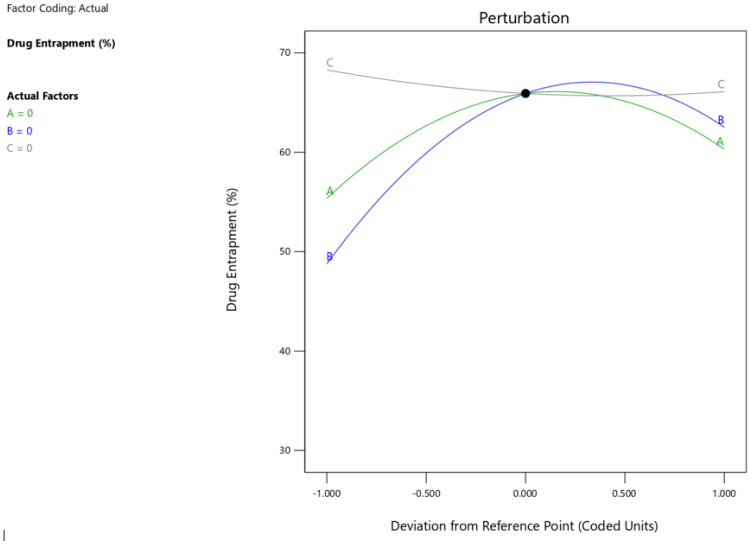

Figure 2 b(ii): Perturbation graph for the effect of all independent variables on % Entrapment Efficiency.

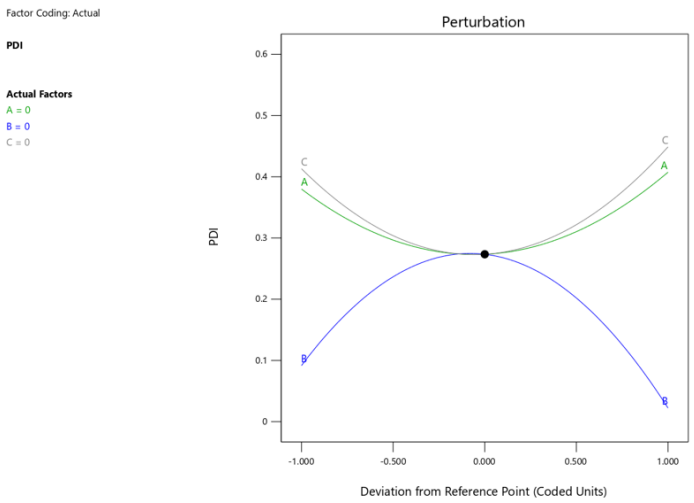

Figure 2 b(iii): Perturbation graph for the effect of all independent variables on Polydispersity Index (PDI).

RESULTS

Analytical statistics

Graph Pad Prism (version 9.0) was used to statistically analyze the data. The ANOVA, or analysis of variance, was employed to compare several groups. In every case, a *p*-value of 0.05 or less was considered significant. Every experiment has been independently replicated. A minimum of three replications were carried out, unless otherwise noted, and the data was presented as Mean±SD and Outcome.

FT-IR evaluation of drug-excipient compatibility

Prior to conducting a compatibility study, FT-IR is employed to detect all drug-excipient relationships within functional groups. Figure 1 shows an overlay plot of the drug-excipient compatibility study as determined by FT-IR spectroscopy. Free OH, CH3, C-O, C=O CH_2, C-F, and C=C are among the reactive functional groups found in POS. Chitosan, on the other hand, contains reaction groups consisting of CO, C-O-C, C-N, -NH_2, and OH groups; lactose has OH, C-O-C, CH_2, -C=O, and OH groups; and HPβCD includes CH, OH, C=C, C=O, and C-O-C groups. Therefore, it is conceivable for the functional groups of the drug and its excipients to physically interact; this will probably happen via the creation of weak hydrogen bonds and weak connections as a result of dipole-dipole interactions, and van der Waals forces attraction, and other factors. But the clear C-F and N-H bands at around 1130 cm^{-1} and 3070 cm^{-1}, respectively, provided evidence of the physical combination of pure POS Since all of the predicted peaks for the drug and the excipient were present in the physical combination and no significant shifting of existing peaks or generation of new peaks was seen, it is likely that there were no chemical interactions between the drug and the excipients.

Analysis of QbD optimization

The goal of this study was to thoroughly examine how process factors affect the formulation. The TPP concentration (mg) (B), stirring speed (rpm) (C), and CS (mg) (A) were among these factors, along with their interactions. Using the Design-Expert DX 13 program, a BBD-an appropriate statistical technique with three factors and three levels-was used to accomplish this. Using a one-way ANOVA with a 0.05 significance level, the variables' significance was evaluated. The Box-Behnken design was specifically chosen because it made the procedure more efficient and needed fewer trial runs than a central composite design. It was simpler to evaluate the experimental data since the Design Expert program created the design matrix using data from seventeen experimental runs.

Table 1 displays the results of the seventeen generated formulations. The 3D response surface plots for the three Y1, Y2, and Y3 responses are displayed on chitosan, Tripolyphosphate and Stirring Speed in Figure 2(a). It is commonly recognized that these diagrams may be used to investigate how two factors together affect a response and to look at how variables and responses interact. Table 2 displays the different ANOVA responses. The larger coefficient's values of standard error supported the interactions' quadratic equations. The response ranges for PS, %EE, and PDI were, in order, 154-334.4 nm, 44-70%, and 0.133-0.573.

Independent variable's impact on particle sizes

A three-dimensional graph displayed the individual and combined independent components impacts on the PS. The particle sizes increased concurrently with an intensification in the CS: TPP ratio. Higher CS concentrations cause the particle size to grow, however it decreases when compared to the CS: TPP ratio. The range of particle sizes for all 17 formulations is 154-334.4 nm. For particle size, the following equation is found. The three-dimensional

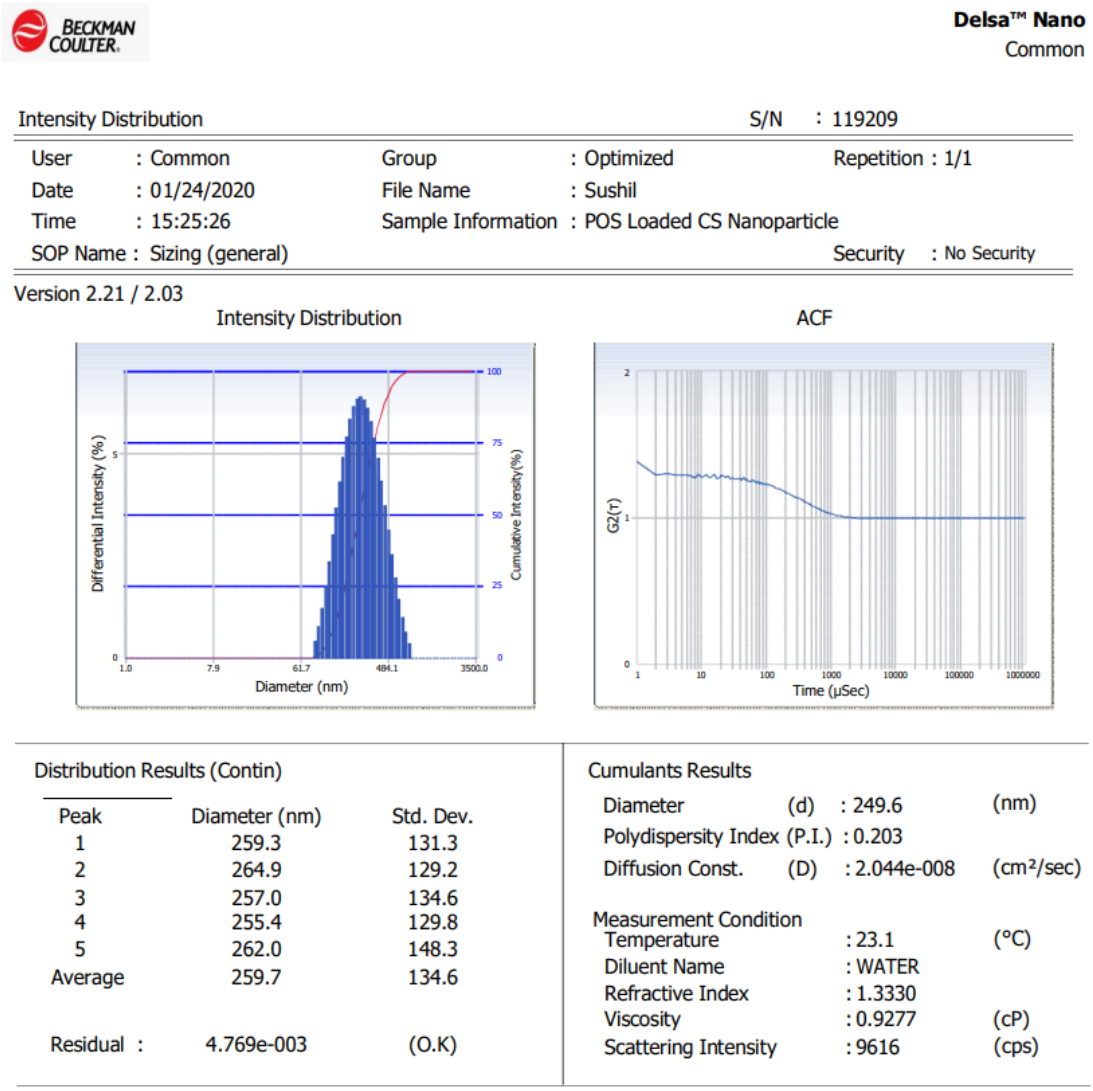

Figure 3a: Size distribution graph of an optimized batch of POS-CSNPs.

surface plot Figure showed the effects of independent parameters, both singular and combined, on the particle size (Y1). Figure's 2(a-i) and the perturbation graph. Figure's 2(b-i). PS=238.48+36.03A+50.33B-8.25C+0.550AB-66.00AC-11.0BC+ 19.08A^2 -13.92B^2 +21.86C^2

The given quadratic equation models the relationship between particle size and variables A, B, and C. It shows both linear and interaction effects. Positive coefficients, like 36.03A and 50.33B, suggest that increasing A or B increases particle size. Negative coefficients, like -66.00AC and -13.92B^2, indicate diminishing effects or reductions in size. Interaction terms (AB, AC, BC) highlight the combined influence of variables, while squared terms reflect non-linearity, revealing complex particle size dependencies.

The graphs and statistics made it abundantly noticeable that the selected parameters significantly affected the particle size. The model F-value of 171.14 (F-value more than 10) and the obtained P-values of the quadratic model less than 0.0500, or 0.0001, show that the model terms are significant. For the quadratic model for particle size, adjusted R^2, or 0.9897, and projected R^2, or 0.9550, had recorded discrepancies of less than 0.2, indicating a significant correlation between the experiment's results and those anticipated. The additional precision, or signal-to-noise ratio greater than 4, or 50.7114, demonstrated sufficient signals were present to follow the design space when assessed with the appropriate precision.

Impact of Independent Factors on % Entrapment Efficiency

Every independent variable has been shown to have an impact on encapsulation efficiency. Figures 2(a-ii) and 2(b-ii) of the perturbation graph and response surface plots, respectively, showed the combined impacts of separate components on EE. It has been shown that the ratio of CS: TPP concentration rises

BECKMAN COULTER

Delsa™ Nano
Common

Distribution Graph S/N : 120909

User	: Common	Group	:	Repetition	: 1/1
Date	: 07/03/2018	File Name	: meraj7318-01_20180307_152448		
Time	: 15:24:48	Sample Information	:		
SOP Name	: VIJAY			Security	: No Security

Version 2.31 / 2.03

Mobility Distribution

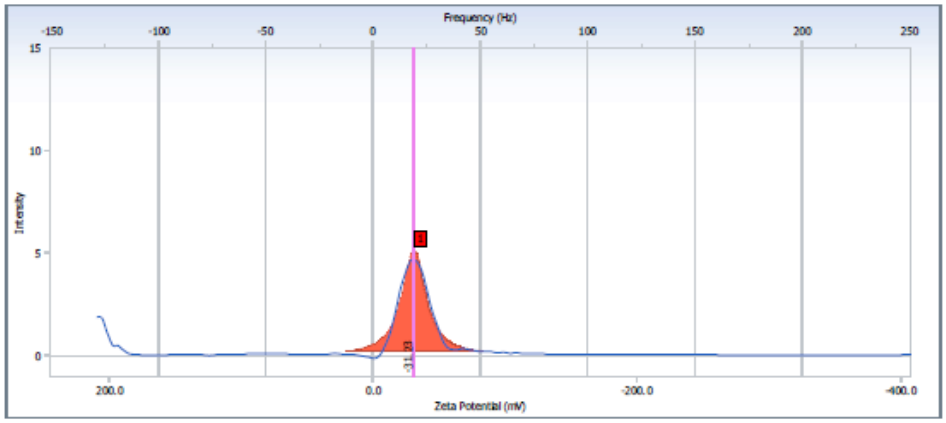

Measurement Results

Zeta Potential	: -31.23	(mV)	Doppler shift	: 19.21	(Hz)
Mobility	: -2.435e-004	(cm²/Vs)	Base Frequency	: 124.6	(Hz)
Conductivity	: 0.0390	(mS/cm)			

Zeta Potential of Cell			Diluent Properties		
Upper Surface	: -8.57	(mV)	Diluent Name	: WATER	
Lower Surface	: -10.61	(mV)	Temperature	: 25.0	(°C)
Cell Condition			Refractive Index	: 1.3328	
Cell Type	: Flow Cell		Viscosity	: 0.8878	(cP)
Avg. Electric Field	: -16.33	(V/cm)	Dielectric Constant	: 78.3	
Avg. Current	: -0.03	(mA)			

Peak Data Table of Distribution Graph

Peak	Frequency (Hz)	Intensity	Half Width (Hz)	Zeta Potential (mV)	Mobility (cm²/Vs)
1	19.21	5.12	6.45	-31.23	-2.435e-004

Figure 3b: Zeta potential graph of POS-CSNPs.

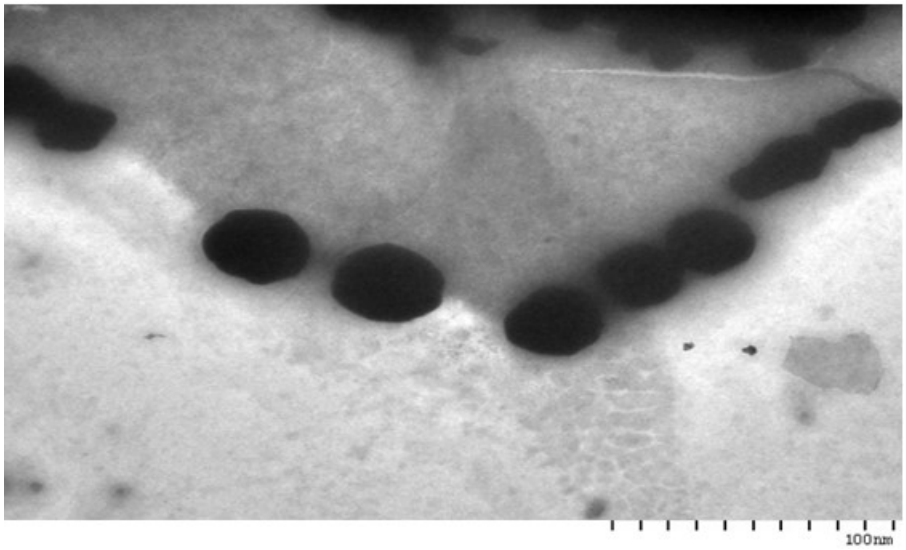

Figure 3c: TEM image of optimized POS-CSNPs.

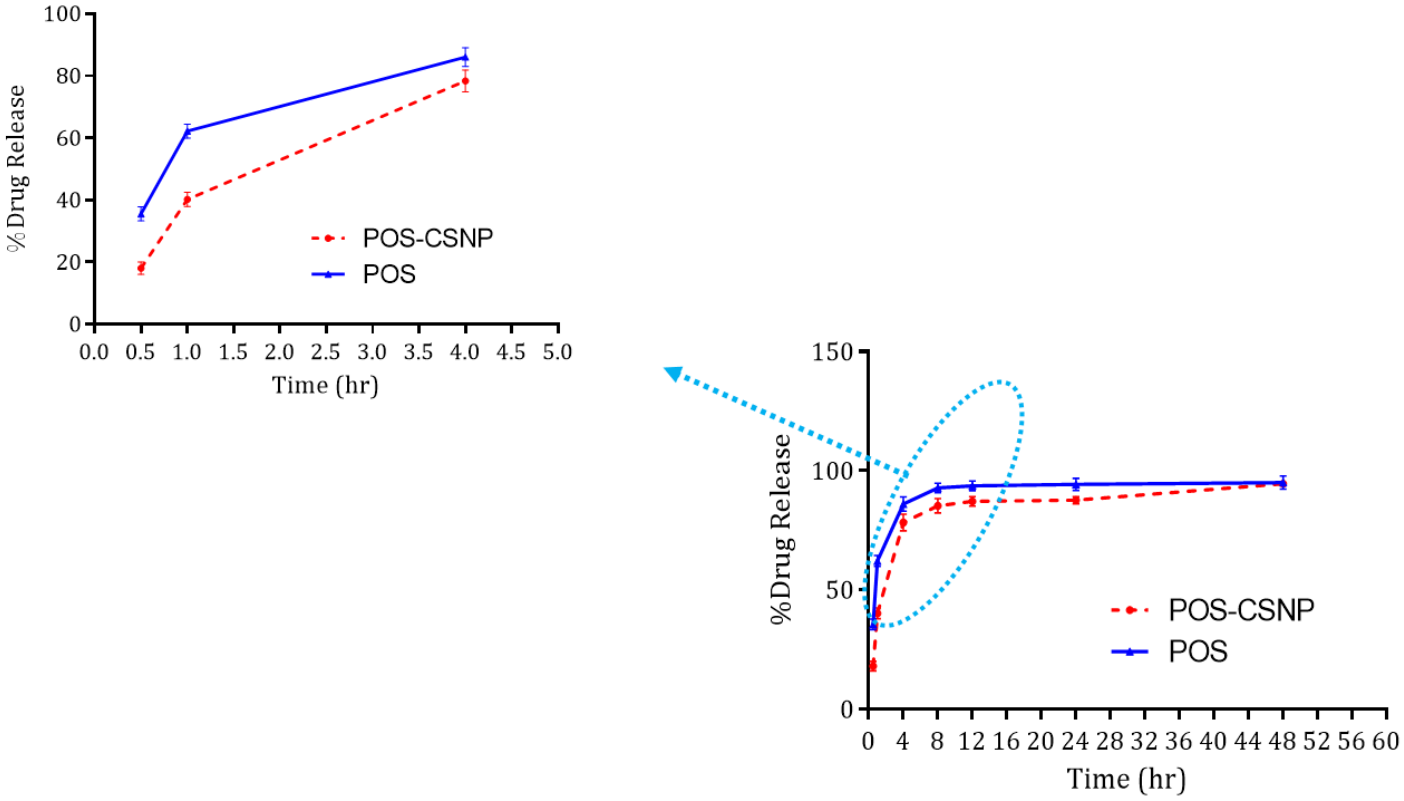

Figure 3c: *In vitro* drug release profile from POS-CS NPs suspension in phosphate buffer (7.4 pH).

along with the entrapment effectiveness of POS-CSNPs. When the speed of stirring is increased, the effectiveness of entrapment also improves; however, it decreases when compared to the ratio of CS: TPP concentration. There is a negative correlation between the stirring speed and entrapment efficiency; a positive correlation exists between the two. EE is calculated by the following equation.

$$\%EE=65.92+2.48A+6.88B-1.10C+0.8250AB+0.8250AC+1.93BC-8.07A2-10.27B2-1.28C2$$

The given quadratic equation models the entrapment efficiency based on variables A, B, and C. The constants (65.92, 2.48, 6.88, etc.) represent coefficients that indicate how each factor contributes to the overall efficiency. Positive terms like 2.48A, 6.88B, and 1.93BC suggest that increasing these variables positively influences the efficiency, while negative terms such as $-8.07A^2$, $-10.27B^2$, and $-1.28C^2$ indicate diminishing returns at higher levels of these factors. The interaction terms (AB, AC and BC) show how combinations of variables affect efficiency. This equation reflects a complex relationship where each factor and their interactions need to be carefully balanced for optimal performance.

The quadratic equations F-value of 26.20 and *p*-value of 0.0001 both show that the terms in the model are important/ significant. Additionally, Adjusted R^2 of 0.9343 and projected R^2 of 0.8085 for the model and quadratic of entrapment efficiency demonstrated changes of less than 0.2, showing a significant connection between the experiment's findings and those predicted. Enough signals were present to track the design space. According to the adequate precision assessment of 15.4630, which is greater than 4.

Independent variable effects on PDI

Every independent variable has been shown to have an impact on the PDI. Regarding the perturbation graph Figure 2(b-iii) and 3D response surface graphs Figure 2(a-iii). The PDI (Y3) of formulation POS-CSNPs was shown to rise with increasing CS concentration. As the concentration of CS: TPP ratio and Stirring speed increases, PDI drops. PDI is calculated by following the equation.

$$PDI=0.2734+0.0138A-0.0346B-0.0179C+0.0107AB-0.0003AC-0.0185BC+0.1203A2-0.2165B2-0.1575C2$$

The given quadratic equation for PDI illustrates the intricate relationships among variables A, B, and C in predicting the dependent variable. The coefficients indicate how each variable and their interactions contribute to PDI. Notably, the positive coefficient for A suggests a direct influence, while the negative coefficients for B and C indicate inverse relationships. The interaction terms (e.g., AB and BC) highlight the complexity of these relationships, showing how combinations of variables affect PDI. The quadratic terms (A^2, B^2, C^2) emphasize the significance of non-linear effects, suggesting that the relationships are not

merely additive but also influenced by the magnitude of each variable.

The quadratic model's F-value of 31.80 and P-value of 0.0001 both show that the model's terms are significant. Additionally, the adjusted R^2 of 0.9454 and the projected R^2 of 0.7691 for the quadratic model for the PDI showed inconsistencies of less than 0.2, showing a strong correlation between the experiment's outcomes and hypotheses. Sufficient signals were available to track the design space, according to adequate precision, or 17.0536, which is larger than 4.

Point prediction

All seventeen formulations' results were suited to multiple kinetic orders.; A quadratic model was the best fit for the optimized formulations. Since each independent variable, both alone and in combination, has a significant influence on the dependent variables, It is highly advised to use the quadratic model for the formulation. A linear relationship was demonstrated between the software-predicted experimental findings and the actual experimental outcomes. The point prediction technique of the software was used to observe the prediction error, which ranged from 0.082 to 0.094. Based on the criteria for the least PS, maximum EE, and maximum PDI, the best formulation of POS-CSNPs was selected.

Particle size, entrapment efficiency, PDI, and Zeta potential

Table 3 lists the PS, PDI, and EE of the improved formulation. Our study's findings indicated that the average particle size of the created formulations was 259.33±6.82 nm. The value of the PDI fell below 0.192±0.010, demonstrating their monodisperse nature. The graph of the improved formulation POS-CSNPs' size distribution graph of an optimized batch is displayed in Figure 3(a). The improved formulation yielded a ZP of -31.23±0.84, zeta potential graph of POS-CSNPs as displayed in Figure 3(b), the graph of zeta potential. It was determined that the optimized formulation POS-CSNPs had a %EE of 65.17±1.71.

Analysis of surface Morphology (TEM)

The morphological data used in the formulation of POS-CSNPs was shown in Figure 3(c) using TEM analysis, under a microscope, a more spherical form was observed. The results demonstrate that the particles were split apart and distributed uniformly, displaying the shape and center of the distinct particles.

In vitro drug release

To examine the *in vitro* release of POS in PBS (pH 7.4) at 37±1°C, the dialysis technique is utilized. Because of the plasma's modeling behavior, pH 7.4 was chosen (Hu, Zhang *et al*. 2020). The analysis indicated that, in comparison to the POS-CSNPs formulation, which had a comparatively quicker release, the POS-CSNPs formulation displayed a more sustained release pattern. Within 48 hr, POS-CSNPs did not exhibit 100% release, but rather exhibited continuous release. At first, the free POS solution indicated that the release was 80% as observed for the 1st 4 hr. However, after that, a gradual release was observed over the next 24 hr, meaning that 65.7±2.4% of POS was released from POS-CSNPs. A study was conducted on the medication release % of POS and POS-CSNPs. Upon completion of the 48-hr experiment, 81.26±2.8% of the POS was liberated from the POS-CSNPs formulation, as seen in Figure 3(d). *In vitro* release patterns were examined using KinetDS3 software which matched

Table 4 (i): Spray-dried microparticles and their particle size distributions (Mean± S.D., *n*=3).

Formulations	Size (µm)		Span
	Median	Mode	
POS-CSNPs+5% lactose	2.74±0.24	2.34±0.19	1.74±0.06
POS-CSNPs+10% lactose	3.14±0.21	2.79±0.10	1.96±0.07
POS-CSNPs+20% lactose	3.42±0.16	2.84±0.08	2.04±0.04

Table 4 (ii): Spray-dried microparticles and their *in vitro* deposition parameters (Mean± S.D., *n*=3).

Formulations	ED %	FPF; %
POS-CSNPs+5% lactose	49.7±3.8	27.7±0.6
POS-CSNPs+10% lactose	37.9±3.5	29.2±1.2
POS-CSNPs+20% lactose	39.5±2.6	26.9±1.3

the data using many plausible kinetic models as indicated by the models of Hixson-Crowell. The model fit well in comparison to other models, indicating that the presence of CS on the surface of POS-CSNPs causes the loaded POS to be released via a non-diffusion mechanism. This might account for the significant variation in drug release that was seen ($p<0.05$).

Studying of X-ray Diffraction (XRD)

Figure 4(a) displays the X-ray diffraction pattern of free drug POS and POS-CS NPs. According to earlier literature investigations, free drug POS exhibits strong peaks around 18.2˚, as shown in Figure 4(a-i). The strong peaks of POS totally vanished in POS-CS NPs, suggesting that the polymer in the formulations molecularly dispersed POS, hence demonstrating the full drug encapsulated seen in Figure 4(a-ii).

DSC thermal analysis

The type of thermogram depicted in Figures 4(b) and 4(c) represents the results acquired from the DSC examination of POS, CS, TPP, HPβCD, Physical mixture, and optimal formulation (POS-CSMPs). According to the graph, Free drug POS exhibits a strong melting endothermic peak at 173.65ºC and a solid-liquid transition between 169.41ºC and 178.05ºC, the prominent peak displays the free drug POS in its crystalline form. The strong endothermic peak of POS was seen to vanish in the physical mixture and optimized formulations (POS-CSMPs), indicating the lack of free POS in the formulation's outer surface. Additionally, it may be said that the drug's complete integration into the formulation's core lessens the peak's sharpness and unifies the drug's POS encapsulation.

Study of *in vitro* pulmonary deposition

In comparison to the similar formulations that were spray-dried with lactose (10% to 20 the dosages of drugs inhaled after the spray-dried, POS-loaded CS nanoparticles aerosolized, from the inhaled and Lactose (5%) was much greater and shown in Table 4. the notable rise in the drug's dosage % that was aerosolized in an *in vitro* experiment when powders containing nanoparticles were used. The results observed for spray-dried powders made with lactose may have a synergistic impact on enhancing the nanoparticles' propensity to aerosolize. When compared to the sample made spray dried samples showed much greater deposition patterns. As a result, it can be concluded that the addition of lactose in very small amounts-as low as 5% w/w with relation to nanoparticle weights-much improves the deposition patterns of the aerosolized nanoparticles. In terms of nanoparticle weight, powders spray dried from an aqueous solution containing 10% w/w lactose showed the greatest FPF of aerosolized medication and smooth surface & depicted in Tables 4 (i) & Table 4 (ii). Van der Waals forces are thought to have a significant impact on the adherence of particles with smooth surfaces. The literature reports on the impact of surface roughness on the aerosolized drug's FPF.

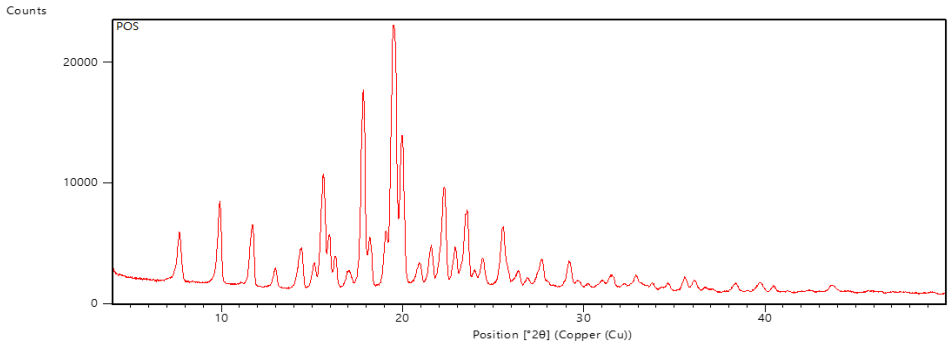

(4.a-i)

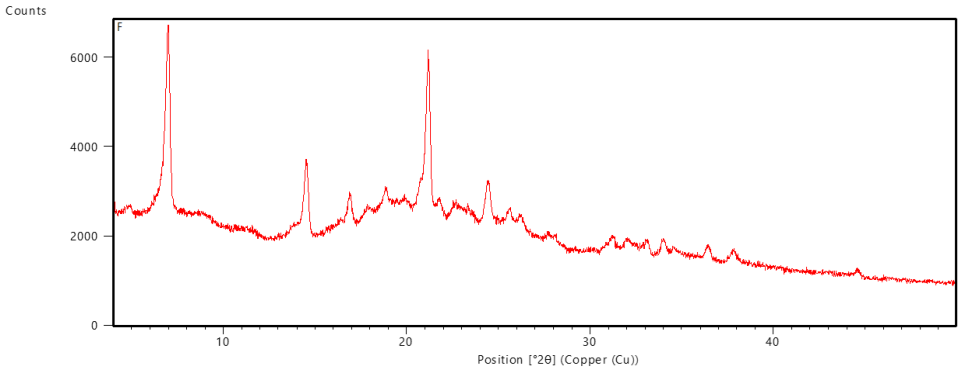

(4.a-ii)

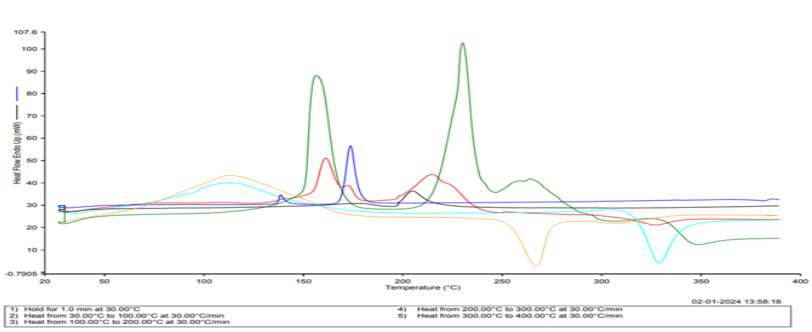

CS	329.18 °C
HPβ-CD	267.28°C
PM	161.20°C
POS	173.63°C
Lactose	230.18°C
TPP	204.95°C

(b)

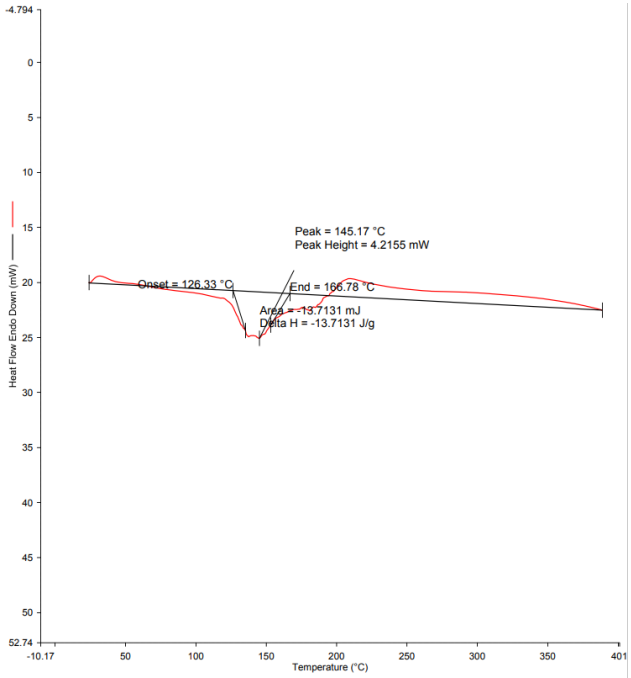

(c)

Figure 4: (4.a-i): XRD spectra of free POS. (4.a-ii): XRD spectra of Optimized Formulation (POS-CSMPs). (b): DSC overlay thermogram of POS, HP-BCD, Lactose, TPP, Physical mixture and Optimised Formulation (POS-CSMPs). (c): DSC overlay thermogram of Optimised Formulation (POS-CSMPs).

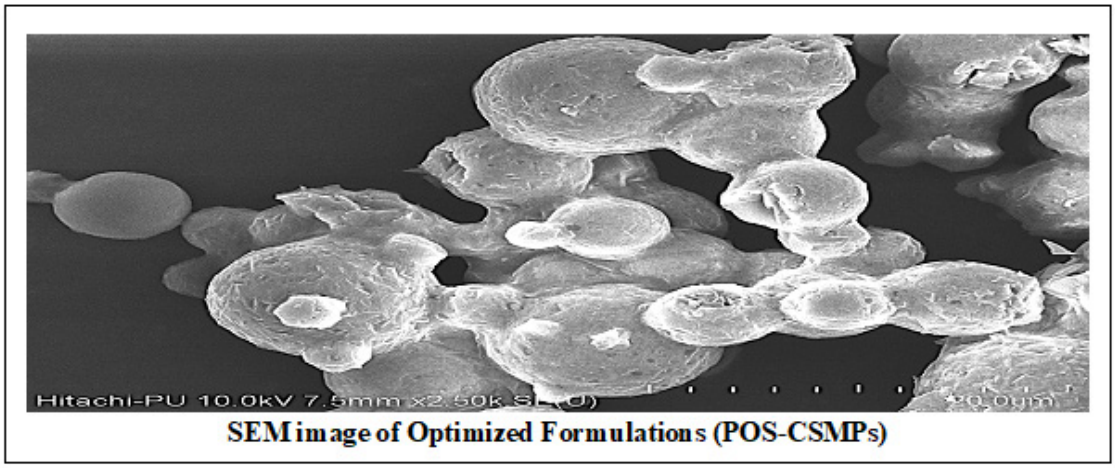

Figure 5: SEM Image.

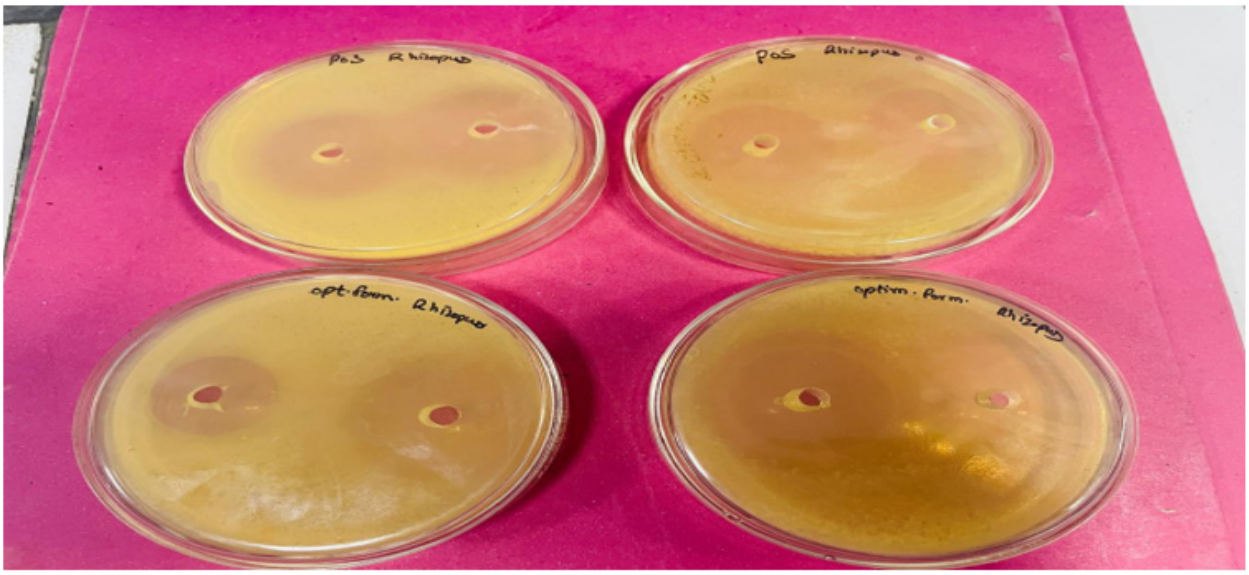

Figure 6: *In vitro* fungal study of Posaconazole (POS) and Optimized Formulations.

Table 5: Accelerated stability condition data for optimized formulation (dry powder).

Parameters	Initial	1 month	3 month
Physical description	White powder	White powder	White powder
Particle size	2.74± 0.24	2.89± 0.14	2.99± 0.18
PDI	0.201±0.006	0.210±0.002	0.220±0.005
% Drug content	29.33±0.12	28.02±0.23	27.91±0.23
% Assay	98.49±0.45	96.86±1.78	96.16±1.62

In vitro antifungal studies

The zone of inhibition (mm) was seen for both the optimized formulation (Rhizopus Oryzae: 20±0.8;) and pure POS (18.2±0.2). Furthermore, it was shown that POS had reduced fungicidal action against pathogenic fungi that cause Rhizopus oryzae. Optimized formulation>POS was shown to be the order of fungicidal action. The antimicrobial activity classification yielded two levels of activity: strong/robust activity if the inhibitory zone diameter (ZI>21 mm) and moderate activity (12 mm<ZI<21 mm). The distance for ZI was classified into three categories based on the antimicrobial activity classification: high activity (ZI>21 mm), and medium (12 mm<ZI<20 mm). The produced optimized formulation was deemed to have the maximum fungicidal activity against the identified Rhizopus (fungal strains), as per the aforementioned assertion.

DISCUSSION

The goal of this work was to develop stable and efficient microparticles for an antifungal medication called POS inhaler delivery. The formulation's properties and potential for fungal therapy were assessed using a variety of analytical methods and optimization procedures. FTIR was used to investigate the drug-excipient compatibility study at the start of the study. The findings suggested, there were no observable interactions among POS and excipients, suggesting a physical combination mostly via Vander Waals forces and weak hydrogen bonds.

After that, Quality by Design (QbD) optimization analysis was used to fully evaluate how process factors affected the formulation. The study employed a Box-Behnken design to effectively investigate the impacts of the concentration ratio of CS: TPP and the stirring speed. The results showed that these parameters had a substantial impact on the Poly Dispersity index (PDI), Entrapment Efficiency (EE), and Particle Size (PS).

The study found a quadratic model for particle size that predicted these factors' effects with accuracy. The findings demonstrated a correlation between the experimental and projected findings, guaranteeing accuracy in the design space. Similar modeling approaches were also used to assess the effect of these factors on PDI and % entrapment efficiency. And data demonstrated excellent correlations between the predicted and experimental outcomes, that both dimensions were significantly impacted by the chosen variables. The improved formulation demonstrated an entrapment effectiveness of 65.5%, a positive zeta potential of 30.2 mV, mono dispersity (PDI < 0.195), and a particle size of around 256 nm.

A spherical shape with distinct particles was found by morphological investigation using TEM, suggesting homogeneous dispersion and encapsulation of POS. The lack of crystalline POS in the formulation was verified by X-ray Diffraction (XRD) and Differential Scanning Calorimetry (DSC) studies, showing effective drug encapsulation within the nanoparticle. Optimized formulations showed slower release patterns with sustained release in drug release trials. The fact that neither formulation

reached 100% release in less than 48 hr suggests that they might be used for regulated medication delivery.

Optimized formulation>POS was shown to have the highest order of fungicidal activity in antifungal experiments utilizing the antifungal activity, which demonstrated that POS-CSMPs had greater fungicidal activity against *in vitro* fungal research. The antimicrobial activity classification yielded two levels of activity: powerful activity if the inhibitory zone diameter (ZI > 21 mm) and moderate/medium activity (12 mm < ZI < 21 mm). The distance for ZI was classified into three categories based on the antimicrobial activity classification: high activity (ZI > 20 mm), moderate/ medium (12 mm < ZI < 21 mm), and lowest/ slow activity.

This study presents a novel POS-CSMPs inhalable formulation, optimized using Quality by Design (QbD) for stable, controlled antifungal drug delivery. Its enhanced entrapment efficiency, sustained release, and superior fungicidal activity highlight its clinical potential for treating pulmonary fungal infections, offering improved efficacy, reduced side effects, and precise drug distribution, making it a promising therapeutic advancement.

The antifungal efficacy and sustained release profile of POS-CSNPs in this study offer significant advantages over conventional formulations reported in the literature, particularly in terms of localized delivery, prolonged retention, and enhanced therapeutic action.

Compared to the formulations discussed by Cheng *et al*., (2020), which highlight the limitations of systemic antifungal treatments including excessive systemic exposure, severe side effects, and poor lung retention POS-CSNPs demonstrate improved drug localization in pulmonary tissues, minimizing systemic toxicity while ensuring sustained drug release. The controlled release profile (>48 hr) of POS-CSNPs ensures that therapeutic drug concentrations remain in the lungs for a prolonged period, unlike conventional formulations that require frequent dosing. Moreover, nanocarrier-based pulmonary delivery, as emphasized by Cheng *et al*., is a promising approach, and POS-CSNPs advance this strategy by offering high entrapment efficiency (65.5%) and optimized particle characteristics (PDI<0.195, 256 nm size), which are crucial for deep lung deposition and effective fungal eradication.

Similarly, in comparison to Brunet *et al*., (2022), who discuss the challenges of systemic antifungal agents (e.g., amphotericin B and triazoles) in treating pulmonary mold infections due to high toxicity and limited dose escalation, POS-CSNPs provide a safer alternative. By using pulmonary inhalation, POS-CSNPs enhance drug concentration at the site of infection while significantly reducing systemic exposure, addressing the critical pharmacokinetic limitations of current antifungal therapies. Additionally, the positive zeta potential (30.2 mV) of POS-CSNPs ensures good stability and bioavailability, potentially improving therapeutic outcomes compared to conventional systemic antifungal regimens.

Overall, the optimized formulation of POS-CSNPs presents a clinically relevant advancement in pulmonary antifungal therapy by providing a superior balance between efficacy and safety. The enhanced fungicidal activity, supported by a well-defined antimicrobial classification (ZI > 21 mm for strong activity), confirms its effectiveness against fungal pathogens. This targeted pulmonary delivery approach represents a substantial improvement over traditional systemic therapies, aligning with the ongoing research emphasis on nanotechnology-based inhalable antifungal treatments.

CONCLUSION

The latest work set out to create a POS-CS microparticle delivery system that was stable and integrated both CS and TPP. When paired with TPP-based nanoparticles for point-of-care administration, the use of CS as an inactive ingredient in the suggested microparticle formulation, which was improved by QbD employing BBD has a lot of potential for drug delivery. Technique for antifungal medications. This plan of action is a very advantageous choice for treating fungus as it can potentially improve both pharmacokinetic and dynamic characteristics and lessen side effects that are frequently linked to fungicidal treatments. The case study showed how the QbD technique works well for improving nanoparticle formulations. It also made it possible to evaluate how process parameters affect critical attributes like PS, %EE, and PDI in the formulation of microparticles. Furthermore, even at lower dosages, the novel formulation demonstrated enhanced antifungal activity against fungus, suggesting that it may find use in the treatment of lung fungal infections. These results are important for developing dry powder systems of surface functionalized/targeted POS-loaded CS microparticles for both clinical and pre-clinical uses. Additionally, the formulation that was found may have the benefit of lowering the frequency of POS medication dosages, which makes it a viable strategy for extra effective and focused drug administration.

ACKNOWLEDGEMENT

Authors are highly thankful to their Universities/ Colleges for providing library facilities for the literature survey. And authors would like to thank Ganpat University, Mehsana India, Spray dryer, UV, HPLC, and ISF College of Pharmacy, Moga, India (ISFAL LAB) for the Spray dryer, DSC, FTIR, Zetasizer, and Fungus study. SAIF, Punjab Agriculture University for TEM, Punjab University, India for XRD facility.

ABBREVIATIONS

Bbd: Box-Behnken Design; **QbD:** Quality by Design; **EE:** Entrapment Efficiency; **IFN-γ:** Interferon gamma; **Cyp51:** Sterol 14α-demethylase; **DPIs:** Dry powder inhalers; **CS:** Chitosan; **POS:** Posaconazole; **TPP:** Tripolyphosphate; **HPβCD:** Hydroxyl propyl-β-cyclodextrin; **ICH:** International Council for Harmonisation; **DoE:** Design of Experimentation; **NPs:** Nanoparticles; **HPLC:** High-Performance Liquid Chromatography; **DSC:** Differential Scanning Calorimeter; **FTIR:** Fourier transform infrared; **RSM:** Response surface methodology; **CCD:** Central Composite Design; **PDI:** Polydispersity Index; **DLS:** Dynamic light scattering; **PBS:** Phosphate-buffered saline; **PS:** Particle size; **ZP:** Zeta potential; **XRD:** X-ray diffraction; **FPF:** Fine particle fraction; **TSI:** Twin-stage impinger apparatus; **ED%:** Emitted dose percentage; **ZI:** Zones of inhibition; **SD:** Standard Deviation; **mg:** Milligram.

CONFLICT OF INTEREST

The authors declare that there is no conflict of interest.

ETHICAL APPROVAL

We conducted no animal activities during this research, and there were no animal or human participants. Therefore, there is no need for ethical approval.

CREDIT AUTHOR STATEMENT

Sushil Kumar Singh: Data curation, original draft preparation, Writing and editing, *in vitro* Data acquisition and evaluation, Visualization, Investigation, **Shyam Sundar Pancholi:** Editing and Proof reading, Conceptualization and Supervision.

CONSENT FOR PUBLICATION

All authors are given their consent for publication. The authors authorized Dr. Shyam Sunder Pancholi for all correspondence.

SUMMARY

In current research, dry powder formulation of POS-CS based microparticles formulated and assessed for the antifungal activity. The QbD-optimized formulation POS-CSNPs exhibits a particle size in the nano range of 259.33±6.82. It also has a PDI of 0.192±0.010, a zeta potential of -31.23±0.84, and a percentage EE of 65.17±1.95. Additionally, it demonstrates superior fungicidal impact and greater antifungal characteristics. The development of targeted POS-loaded CS microparticle systems for pre-clinical and their clinical applications would benefit from these findings. The newly found formulation is a potential strategy for more effective and focused medication delivery since it may also have the benefit of lowering the frequency of POS drug dosages.

REFERENCES

1. Chavda VP, Apostolopoulos V. Mucormycosis-an opportunistic infection in the aged immunocompromised individual: a reason for concern in COVID-19. Maturitas. 2021; 154: 58-61.
2. Pan J, Tsui C, Li M, Xiao K, de Hoog GS, Verweij PE, *et al.* First case of rhinocerebral mucormycosis caused by Lichtheimia ornata, with a review of Lichtheimia infections. Mycopathologia. 2020; 185: 555-67.
3. Skiada A, Pavleas I, Drogari-Apiranthitou M. Epidemiology and diagnosis of mucormycosis: an update. Journal of fungi. 2020; 6(4): 265.
4. Darwish RM, AlMasri M, Al-Masri MM. Mucormycosis: the hidden and forgotten disease. Journal of applied microbiology. 2022; 132(6): 4042-57.
5. Koltsida G, Zaoutis T. Fungal lung disease. Paediatric Respiratory Reviews. 2021; 37: 99-104.
6. Gupta AK, Talukder M, Shemer A, Galili E. Safety and efficacy of new generation azole antifungals in the management of recalcitrant superficial fungal infections and onychomycosis. Expert Review of Anti-infective Therapy. 2024(just-accepted).
7. Mauro M, Colombini A, Perruccio K, Zama D, D'amico MR, Calore E, *et al.* Posaconazole delayed-release tablets in paediatric haematology-oncology patients. Mycoses. 2020; 63(6): 604-9.
8. Shafiei M, Peyton L, Hashemzadeh M, Foroumadi A. History of the development of antifungal azoles: A review on structures, SAR, and mechanism of action. Bioorganic chemistry. 2020; 104: 104240.
9. Dos Santos AR, Fraga-Silva TF, de Fátima Almeida-Donanzam D, Dos Santos RF, Finato AC, Soares CT, *et al.* IFN-γ mediated signaling improves fungal clearance in experimental pulmonary mucormycosis. Mycopathologia. 2022: 1-16.
10. Han G, Liu N, Li C, Tu J, Li Z, Sheng C. Discovery of novel fungal lanosterol 14α-demethylase (CYP51)/histone deacetylase dual inhibitors to treat azole-resistant candidiasis. Journal of medicinal chemistry. 2020; 63(10): 5341-59.
11. McCann S, Sinha J, Wilson WS, McKinzie CJ, Garner LM, Gonzalez D. Population Pharmacokinetics of Posaconazole in Immune-Compromised Children and Assessment of Target Attainment in Invasive Fungal Disease. Clinical Pharmacokinetics. 2023; 62(7): 997-1009.
12. Panagopoulou P, Roilides E. Evaluating posaconazole, its pharmacology, efficacy and safety for the prophylaxis and treatment of fungal infections. Expert Opinion on Pharmacotherapy. 2022; 23(2): 175-99.
13. Cheng SN, Tan ZG, Pandey M, Srichana T, Pichika MR, Gorain B, *et al.* A critical review on emerging trends in dry powder inhaler formulation for the treatment of pulmonary aspergillosis. Pharmaceutics. 2020; 12(12): 1161.
14. Brunet K, Martellosio J-P, Tewes F, Marchand S, Rammaert B. Inhaled antifungal agents for treatment and prophylaxis of bronchopulmonary invasive mold infections. Pharmaceutics. 2022; 14(3): 641.
15. Sethi SK, Goel H, Chawla V. Nanoemulsion Based Supramolecular Drug Delivery Systems for Therapeutic Management of Fungal Infections. Drug Delivery Letters. 2024; 14(1): 2-15.
16. Sousa F, Ferreira D, Reis S, Costa P. Current insights on antifungal therapy: Novel nanotechnology approaches for drug delivery systems and new drugs from natural sources. Pharmaceuticals. 2020; 13(9): 248.
17. Tyagi S, Mani S. Process parameter optimization of vitamin D3 loaded Chitosan-TPP nanoparticles. Materials Today: Proceedings. 2023; 76: 453-8.
18. Pedroso-Santana S, Fleitas-Salazar N. Ionotropic gelation method in the synthesis of nanoparticles/microparticles for biomedical purposes. Polymer International. 2020; 69(5): 443-7.
19. Ebrahimnejad P, Rezaeiroshan A, Babaei A, Khanali A, Aghajanshakeri S, Farmoudeh A, *et al.* Hyaluronic Acid-Coated Chitosan/Gelatin Nanoparticles as a New Strategy for Topical Delivery of Metformin in Melanoma. BioMed Research International. 2023; 2023(1): 3304105.
20. Yee Kuen C, Masarudin MJ. Chitosan nanoparticle-based system: A new insight into the promising controlled release system for lung cancer treatment. Molecules. 2022; 27(2): 473.
21. Chan HW, Chow S, Zhang X, Zhao Y, Tong HHY, Chow SF. Inhalable nanoparticle-based dry powder formulations for respiratory diseases: challenges and strategies for translational research. AAPS PharmSciTech. 2023; 24(4): 98.
22. Kumbhar P, Kaur J, De Rubis G, Paudel KR, Prasher P, Patel VK, *et al.* Inhalation drug delivery in combating pulmonary infections: Advances and challenges. Journal of Drug Delivery Science and Technology. 2023; 89: 105022.
23. Cazzola M, Cavalli F, Usmani OS, Rogliani P. Advances in pulmonary drug delivery devices for the treatment of chronic obstructive pulmonary disease. Expert opinion on drug delivery. 2020; 17(5): 635-46.
24. Mikušová V, Mikuš P. Advances in chitosan-based nanoparticles for drug delivery. International journal of molecular sciences. 2021; 22(17): 9652.
25. de Almeida Campos L, Fin MT, Santos KS, de Lima Gualque MW, Freire Cabral AKL, Khalil NM, *et al.* Nanotechnology-based approaches for voriconazole delivery applied to invasive fungal infections. Pharmaceutics. 2023; 15(1): 266.
26. Ter Horst JP, Turimella SL, Metsers F, Zwiers A. Implementation of Quality by Design (QbD) principles in regulatory dossiers of medicinal products in the European Union (EU) between 2014 and 2019. Therapeutic innovation and regulatory science. 2021; 55: 583-90.
27. Kim EJ, Kim JH, Kim M-S, Jeong SH, Choi DH. Process analytical technology tools for monitoring pharmaceutical unit operations: a control strategy for continuous process verification. Pharmaceutics. 2021; 13(6): 919.
28. Machado JCB, Ferreira MRA, Soares LAL. Optimization of the drying process of standardized extracts from leaves of Spondias mombin L. using Box-Behnken design

and response surface methodology. Journal of Food Processing and Preservation. 2021; 45(7): e15595.
29. Adeyeye MC, Brittain H. Drug-excipient interaction occurrences during solid dosage form development. DRUGS AND THE PHARMACEUTICAL SCIENCES. 2008; 178: 357.
30. Liu H, Guo S, Wei S, Liu J, Tian B. Pharmacokinetics and pharmacodynamics of cyclodextrin-based oral drug delivery formulations for disease therapy. Carbohydrate Polymers. 2024: 121763.
31. Algharib SA, Dawood A, Zhou K, Chen D, Li C, Meng K, *et al.* Preparation of chitosan nanoparticles by ionotropic gelation technique: Effects of formulation parameters and *in vitro* characterization. Journal of Molecular Structure. 2022; 1252: 132129.
32. Emami J, Mohiti H, Hamishehkar H, Varshosaz J. Formulation and optimization of solid lipid nanoparticle formulation for pulmonary delivery of budesonide using Taguchi and Box-Behnken design. Research in pharmaceutical sciences. 2015; 10(1): 17-33.
33. Goyal AK, Garg T, Rath G, Gupta UD, Gupta P. Development and characterization of nanoembedded microparticles for pulmonary delivery of antitubercular drugs against experimental tuberculosis. Molecular Pharmaceutics. 2015; 12(11): 3839-50.
34. Nazari F, Ghoreishi SM, Khoobi A. Bio-based Fe3O4/chitosan nanocomposite sensor for response surface methodology and sensitive determination of gallic acid. International Journal of Biological Macromolecules. 2020; 160: 456-69.
35. Fridman H, Volokh M, Mokari T. Dynamics of the nanocrystal structure and composition in growth solutions monitored by in situ lab-scale X-ray diffraction. Nanoscale. 2021; 13(45): 19076-84.
36. Pettarin M, Bolger MB, Chronowska M, Kostewicz ES. A combined *in vitro in silico* approach to predict the oral bioavailability of borderline BCS Class II/IV weak base albendazole and its main metabolite albendazole sulfoxide. European Journal of Pharmaceutical Sciences. 2020; 155: 105552.
37. Hu C, Zhang F, Long L, Kong Q, Luo R, Wang Y. Dual-responsive injectable hydrogels encapsulating drug-loaded micelles for on-demand antimicrobial activity and accelerated wound healing. Journal of controlled release. 2020; 324: 204-17.
38. Malamatari M, Charisi A, Malamataris S, Kachrimanis K, Nikolakakis I. Spray drying for the preparation of nanoparticle-based drug formulations as dry powders for inhalation. Processes. 2020; 8(7): 788.
39. Jafarinejad S, Gilani K, Moazeni E, Ghazi-Khansari M, Najafabadi AR, Mohajel N. Development of chitosan-based nanoparticles for pulmonary delivery of itraconazole as dry powder formulation. Powder Technology. 2012; 222: 65-70.
40. Omer HK, Hussein NR, Ferraz A, Najlah M, Ahmed W, Taylor KM, *et al.* Spray-dried proliposome microparticles for high-performance aerosol delivery using a monodose powder inhaler. AAPS PharmSciTech. 2018; 19: 2434-48.
41. Eedara BB, Bastola R, Das SC. Dissolution and absorption of inhaled drug particles in the lungs. Pharmaceutics. 2022; 14(12): 2667.Iudicello A, Genovese F, Strusi V, Dominici M, Ruozi B. Development and validation of a new storage procedure to extend the in-use stability of azacitidine in pharmaceutical formulations. Pharmaceuticals. 2021; 14(9): 943.
42. McMahon ME, Abbott A, Babayan Y, Carhart J, Chen C-w, Debie E, *et al.* Considerations for updates to ICH Q1 and Q5C stability guidelines: Embracing current technology and risk assessment strategies. The AAPS journal. 2021; 23: 1-9.
43. Kedar T, Jalalpure S, Kurangi B, Kazi T. Development and validation of stability-indicating RP-HPLC method for the estimation of fisetin in novel cubosomal nanoformulation: Application to the marketed formulation and selected plant extracts. Current Pharmaceutical Analysis. 2022; 18(10): 983-92.

Cite this article: Singh SK, Pancholi SS. Design and Development of Chitosan-Based Posaconazole Loaded Dry Powder by Using BBD. Indian J of Pharmaceutical Education and Research. 2026;60(2s):s443-s461.

Supplementary Table 1: The solubility of various amounts of POS in the presence of the constant amount of HPβCD (Mean± S.D., *n*=3).

POS: HPβCD weight ratio	Solubility (%)
1.0: 50	99.56±1.95
1.5:50	96.33±1.3
2.0:50	92.00±2.3

Supplementary Table 2: Variables and their levels of Box-Behnken design.

Variables	Level		
	Low (-1)	Medium (0)	High (+1)
Independent Variables			
X1=CS (%)	1	2	3
X2=TPP (%)	0.5	1	1.5
X3=Stirring Speed (rpm)	Slow (400)	Medium (800)	Fast (1200)
Dependent Variables	Desirability	Remark: CS-Chitosan TPP-Tripolyphosphate PDI-Polydispersity Index	
Particle size (PS)	Minimum		
% Entrapment efficiency	Maximize		
PDI	Minimum		

Supplementary Table 3: Process Conditions of Spray drying.

Process parameter	Limit
Inlet temperature	120°C
Spraying air flow rate	550 L/hr
Aspiration	80%
Feed rate	2.9 mL/min